Earth Surface Processes and Landforms
Earth Surf. Process. Landforms **27**, 269–288 (2002)
Published online in Wiley InterScience (www.interscience.wiley.com). DOI: 10.1002/esp.318

A CELLULAR MODEL OF HOLOCENE UPLAND RIVER BASIN AND ALLUVIAL FAN EVOLUTION

T. J. COULTHARD,[1]* M. G. MACKLIN[1] AND M. J. KIRKBY[2]

[1] *Institute of Geography and Earth Sciences, University of Wales, Aberystwyth, Ceredigion, SY23 3DB, UK*
[2] *School of Geography, University of Leeds, Leeds, LS2 9JT, UK*

Received 14 August 2000; Revised 30 November 2001; Accepted 12 December 2001

ABSTRACT

The CAESAR (Cellular Automaton Evolutionary Slope And River) model is used to simulate the Holocene development of a small upland catchment (4·2 km^2) and the alluvial fan at its base. The model operates at a 3 m grid scale and simulates every flood over the last 9200 years, using a rainfall record reconstructed from peat bog wetness indices and land cover history derived from palynological sources.

Model results show that the simulated catchment sediment discharge above the alluvial fan closely follows the climate signal, but with an increase in the amplitude of response after deforestation. The important effects of sediment storage and remobilization are shown, and findings suggest that soil creep rates may be an important control on long term (>1000 years) temperate catchment sediment yield. The simulated alluvial fan shows a complex and episodic behaviour, with frequent avulsions across the fan surface. However, there appears to be no clear link between fan response and climate or land use changes suggesting that Holocene alluvial fan dynamics may be the result of phases of sediment storage and remobilization, or instabilities and thresholds within the fan itself. Copyright © 2002 John Wiley & Sons, Ltd.

KEY WORDS: CAESAR; cellular; model; river; basin; alluvial fan

INTRODUCTION

During the late Holocene there is widespread evidence of morphological change in upland river systems of the UK. Previous studies (e.g. Macklin *et al*., 1992; Macklin and Lewin, 1993; Harvey, 1996; Rumsby and Macklin, 1996; Ballantyne and Whittington, 1999; Merrett and Macklin, 1999; Macklin, 1999) have linked periods of upland river erosion and deposition to wetter past climates and the human removal of forest cover. But although these studies have been very informative, dating control is usually not precise enough to establish unequivocally a direct relationship between environmental change and river response. These links between cause and effect are important as upland catchments can generate large volumes of sediment causing downstream aggradation and channel instability, as well as representing considerable hazards to local inhabitants. Therefore, if we can understand how upland catchments have reacted to previous environmental changes, we can use this information to re-evaluate and devise appropriate management strategies, as well as forecast how upland rivers may respond to future climate changes.

Recently, numerical catchment-wide modelling has begun to answer some of these questions, with models exploring the relationship between climate, land use and sediment discharge on small catchments over periods up to 100 years (Coulthard *et al*., 1999, 2000). These simulations have shown that doubling the rainfall magnitude or removing tree cover can produce increases of 110 and 80 per cent respectively in sediment discharge. But when combined, they generate a 1300 per cent rise in sediment production. Therefore, removing vegetation cover drastically increases catchment sensitivity to climate change. However, these simulations failed to account for three factors that may become important when looking over longer time scales. The first

* Correspondence to: T. J. Coulthard, Institute of Geography and Earth Sciences, University of Wales, Aberystwyth, Ceredigion, SY23 3DB, UK. E-mail: T.Coulthard@aber.ac.uk
Contract/grant sponsor: Natural Environment Research Council; Contract/grant number: GT4/95/147/F.

is periods of climatic transition and the history of flood events; for example, if there is a change to a wetter climate with greater flood magnitudes after a long period of drier weather, the catchment may produce a high sediment discharge, as slope processes have led to the accumulation of sediment on the valley floor or near the channel. Conversely if a period of high flood magnitude follows a wet period, the valley floor and slopes may have been starved of sediment following the previous floods. Second, the previous simulations modelled only nine scenarios of set rainfall magnitudes and land covers, whereas during the Holocene these factors varied continuously. Third, these simulations modelled only periods up to 100 years, and over longer time scales processes such as soil creep may become more important. Therefore, there is a need to understand how process interactions over the Holocene, driven by climate and land-cover changes, affect sediment delivery and catchment evolution.

Within river systems, alluvial fans can act as important controls on sediment transfer. They operate as the interface between upland catchments where sediment is produced, and trunk rivers or sedimentary basins where material is moved and stored. They can switch from being sediment stores when aggrading, to becoming sources when incising, or they may have little influence, delivering sediment directly to downstream areas. Changes in alluvial fan behaviour have been linked to three groups of factors (Harvey, 1997). First, there are changes in base level. Second, controls on water and sediment inputs to the fan have been related to land-use changes (Harvey and Renwick, 1987; Ballantyne, 1991) and to increases in flood magnitude and frequency associated with climate change (Merrett and Macklin, 1999). Third, there are factors controlling sediment transport within the fan itself. For example, a steep single channel is more likely to erode, whereas a distributed branching channel on a shallow gradient is more likely to deposit. Furthermore there may be rapid short-term fluctuations between erosion and deposition along the channel(s) within the fan. However, the individual importance of these three factors is undetermined, as they often work in combination and can have variable impacts in different environments. This leaves us with an incomplete understanding of alluvial fan evolution and how this affects sediment delivery to downstream areas. Therefore, modelling the causes and effects of these factors could help us to better understand fan evolution.

This paper addresses these issues by using a cellular model called CAESAR (Cellular Automaton Evolutionary Slope And River) to simulate the Holocene evolution of a small upland catchment and the alluvial fan at its outlet. Utilising climate and land-cover reconstructions, every flood in the last 9200 years is simulated and used to evaluate how the long-term interactions between climate, land use and sediment supply affect catchment sediment discharge and alluvial fan development.

METHODOLOGY AND MODEL DESCRIPTION

Recently, a number of workers have used catchment-based computer models to study river sediment transport processes and drainage basin development. These have represented hill slopes and river channels through a regular grid of square or hexagonal cells (e.g. Kirkby, 1987; Howard, 1994; Tucker and Slingerland, 1994; Willgoose *et al*., 1994) or irregular mesh of nodes and links (Braun and Sambridge, 1997; Tucker *et al*., 2001). They then alter the elevations of the nodes or grid cells according to approximations for material gains and losses from slope and fluvial processes. These have proved successful, but two key areas have hindered development: first, the representation of channel flow; and second, how to represent and integrate catchment processes that operate over a wide range of spatial and temporal scales.

Channel flow

Within a catchment, water flows from the highest to the lowest point, so within these models any precipitation or flow must be routed from the highest grid cell or node, down to the lowest. Computationally, the simplest method is to sort all the grid cells or nodes within the catchment by elevation, and then work down through the list. For example, if we have a simple grid of 100 by 100 cells, 10 000 points have to be sorted, and if we allow the elevations to change through erosion and deposition, these cells have to be reordered for every iteration. Computationally this sorting can be time-consuming, restricting the number of grid cells, and therefore the area and number of model iterations that can be studied. To resolve this, authors have used a

technique such as the 'bucket passing algorithm' (Braun and Sambridge, 1997) where each node is given a 'bucket' or set amount of water and asked to pass it to its lowest neighbour. After this, all nodes that have not received any water are local 'maxima' and are placed at the top of a list. This process continues until all nodes have been accounted for, resulting in an ordered list. Whilst being significantly quicker, these solutions are only partial, as they require all water to flow in only one direction – that of the steepest descent. At first glance this may be considered a reasonable approximation, but rivers and drainage networks are full of features characterized by divergent channel flow, for example mid-channel bars, alluvial fans and deltas. As Howard (1994) acknowledges when simulating fan and escarpment development: 'owing to the limitation of flow in one of the eight directions at each cell, the fan assumes a prismatic shape during its growth'. In order to fully capture the dynamics of fluvial behaviour a multiple flow algorithm that permits flow in all possible directions is required.

There are two notable exceptions to these single-flow-direction models. First, Moglen and Bras (1995), use a multiple-flow algorithm, but only on a small (40 by 40) grid. Secondly, Murray and Paola (1994, 1997) developed a novel solution for simulating braided rivers. They used a square grid to represent a reach or section of braided river and assumed that there was flow in one main direction (the direction of the valley floor). Water was then added to cells at the top row of the reach and routed to the three cells immediately downstream in the second row, according to the local bed slope. The model then moved onto this second row and routed flow to the three downstream cells in row 3 and so on, in effect pushing the flow down through the reach. This simulated the flow in a braided reach with both divergent and convergent flow. Unfortunately, there are problems associated with their approach, as it failed to calculate a flow depth and only routes water in one main direction, making it unsuitable for drainage basin simulations or complex channel sections (e.g. meanders).

The model described here uses a 'scanning' algorithm that incorporates the simplicity of the Murray and Paola method but allows calculation of flow in all directions. It operates on a square grid, and is illustrated schematically in Figure 1. Here there is a small V-shaped valley where the dark dots represent precipitation added to each grid cell. For every iteration, the procedure uses four scans. The first scan (box 1) operates from left to right, pushing water from grid cells to the three lower cells on the right. When the base of the valley is reached the scan proceeds up the right valley wall, but as the cells are all upslope, no flow is routed to them (as per box 2). On the second scan (box 3), the same process is repeated but here working from right to left, leaving all the water from the catchment in the base of the valley. This is routed by a third scan from top to bottom, pushing all the water out of the catchment (box 4). A fourth scan then operates from bottom to top, but for clarity is not shown here. For each scan, the maximum flow through each point is recorded and taken as the discharge for that point. If the three 'downstream' cells are all higher than the contributing cell, but the combined water depth and elevation of the contributing cell is higher, water is retained in the contributing cell up to the depth of the obstruction whilst the rest is routed on. This process has the effect of filling hollows that the model may create with water ready for the next iteration. These hollows or sinks frequently have to be removed from DEM data (Goodchild and Mark, 1987; Hutchinson, 1989). This water 'trapped' within the topography also allows this scanning method to simulate flow around a series of complex bends or channel geometries. For instance, in a meander sequence, water may be routed around a first corner, but be trapped by a second. However, in the next iteration, this water is still there, to be released in the next scan, and replaced by more water from upstream, allowing the continuum of flow. This method gives very similar results to those from multiple flow algorithms but takes a fraction of the time. This speed has allowed CAESAR to be applied to large grids with over a million cells, but still use a multiple flow algorithm.

Process representation

Within a drainage basin there are a large number of processes operating over a wide range of spatial and temporal scales, and integrating these within one model can prove difficult. For instance, the complex topography of a braided river channel will require a far higher level of spatial detail than a bare hill slope. Furthermore, parameterization of these processes is especially difficult as their importance can vary over both different time and space scales. For instance, soil creep may be inconsequential when simulating a series of floods, but very important when modelling temperate catchment evolution over thousands of years.

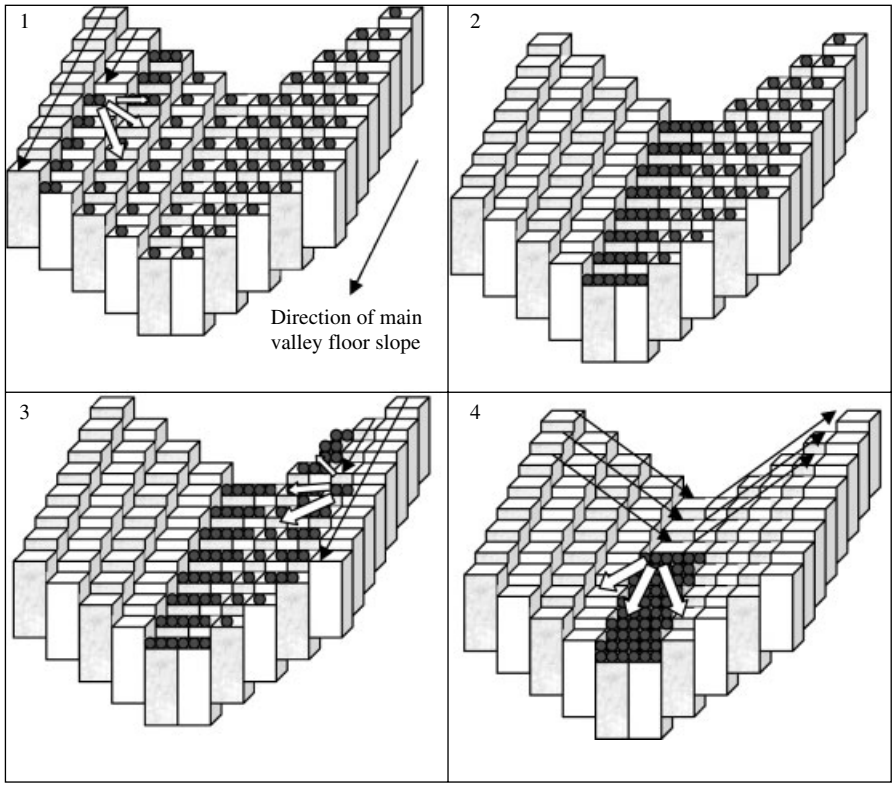

Figure 1. Schematic diagram of the CAESAR scanning flow routing algorithm

Conversely, the location of channel bars may prove important for the single flood but less so over longer periods. Previous workers have used a variety of techniques to address these problems. Braun and Sambridge (1997) and Tucker *et al*. (2001) have used an irregular grid with nodes and links to represent the topography, so areas where more detail is required (e.g. river channels) have more nodes and thus more detail than relatively uniform areas (e.g. a hill slope). Other authors (Howard, 1994; Tucker and Slingerland, 1994) have used sub-grid-scale representation of processes, where for example a small river channel (10 m wide) is represented within a larger (50 m) grid cell, and erosion and deposition averaged across the whole cells area. To cope with long-term studies, most models use averages of erosion rates and long time steps that range from years to decades. The danger of such averaging is that the importance of large individual events may be blurred.

Here, a different approach is taken. The previously described routing algorithm allows a large number of smaller grid cells to be used, which reduces the need for sub-grid-scale representation. This lets a river channel occupy a space one or more cells wide, permitting a more detailed simulation of the channel bed topography, including alluvial features such as channel bars, terraces and alluvial fans. CAESAR is optimized by concentrating on cells where fluvial processes dominate, yet periodically checking hill slopes. This procedure involves routing an initial set discharge down the catchment, noting which cells are 'wet' and setting a five-cell buffer around this area. Then, for every iteration, fluvial erosion, deposition and local slope processes are calculated within this 'buffer zone', and every 100 iterations the entire catchment is checked. If during a flood the discharge exceeds 50 per cent of the set discharge used to calculate the buffer zone, this discharge is doubled and the buffer area recalculated. This allows the drainage network to expand or contract during a flood whilst optimizing the number of cells examined. In addition, a variable time step is used which is related to the volume of erosion and/or deposition. This can reduce the time step to fractions of a second during a flood yet increase it to a maximum of 30 minutes during low-flow situations. This means that the model simulates entire floods with rising and falling stages, instead of averaging over a single storm

or several events. CAESAR also counts both iterations and time elapsed during the simulation, which allows certain processes (e.g. soil creep) to be calculated every simulated month, while others that may be more dependent on the erosion activity (e.g. landslides) are determined every set number of iterations.

MODEL OPERATION

Using the optimizations described above, the model integrates five groups of processes. The following sections describe in detail how they operate and are implemented.

Hydrological model

A modification of TOPMODEL (Beven and Kirkby, 1979) is used to generate a combined surface and subsurface discharge (Q_{tot}) for cells within the buffer zone. This is calculated according to Equation 1, where T is the time step (in seconds), r the rainfall rate (in $m^{-1}h^{-1}$) and m is a parameter that controls the rise and fall of the soil moisture store (j_t) that is calculated from the value of j_t in the previous iteration (j_{t-1}). m is derived from the recession curve of the flood hydrograph (Beven, 1997).

$$Q_{tot} = \frac{m}{T} \log \left(\frac{(r - j_t) + j_t \exp\left(\frac{rT}{m}\right)}{r} \right)$$
$$j_t = \frac{r}{\left(\frac{r - j_{t-1}}{j_{t-1}} \exp\left(\left(\frac{(0-r)T}{m}\right) + 1\right)\right)} \quad (1)$$

If there is no precipitation ($r = 0$) then Equation 2 is used:

$$Q_{tot} = \frac{m}{T} \log \left(1 + \left(\frac{j_t T}{m}\right)\right)$$
$$j_t = \frac{j_{t-1}}{1 + \left(\frac{j_{t-1} T}{m}\right)} \quad (2)$$

Cells at the edge of the buffer zone may receive water from outside of this area, and to account for this, the discharge (Q_{tot}) for these cells is multiplied by the drainage area (the area of grid cells that the cell receives water from), which in turn is determined during the buffer zone calculation.

Discharge routing

For each cell within the buffer zone, a simple runoff threshold is calculated (Equation 3) which is based upon the amount of water that will infiltrate through the soil, a balance of the hydraulic conductivity (K), the slope (S) and the horizontal spacing or size of grid cell (Dx):

$$Threshold = KS(Dx)^2 \quad (3)$$

This is then subtracted from Q_{tot} and the amount above is treated as runoff, that below as subsurface flow. The subsurface flow is routed using the previously described scanning routine, and the proportion routed to the three receiving cells is calculated with Equation 4. Here Q_i is the fraction of discharge delivered to the neighbouring cell i from the total subsurface flow (Q_{sub}, in m^3s^{-1}), according to the slope S between the cell and its relative neighbours i(numbering from one to three). Differences in slope between diagonal neighbours are accounted for by dividing by $\sqrt{2(Dx^2)}$.

$$Q_i = Q_{sub} \frac{S_i}{\sum S_i} \quad (4)$$

With the surface flow fraction, the depth is calculated using a rearrangement of Manning's equation (Equation 5):

$$Q = \frac{A(R^{0.67}S^{0.5})}{n} \tag{5}$$

where A is cross-sectional area, R is hydraulic radius, S is slope and n is Manning's coefficient. This can be rearranged to give Equation 6, with width (w) as Dx, leaving depth (d):

$$d = \left(\frac{Qn}{S^{0.5}}\right)^{3/5} \tag{6}$$

Very low slopes can result in excessive depths being calculated. To account for this, when the slope is less than 0·005, the depth is set to the same value as discharge.

Surface water is then routed in a similar fashion to Equation 4, except the depth of water as well as cell elevation is considered:

$$Q_i = Q_{surf}\frac{[(e+d)-e_i]}{\sum[(e+d)-e_i]} \tag{7}$$

Here Q_{surf} is the total surface discharge in the cell, e is the elevation and d depth of water (in metres) for each neighbouring cell i. The maximum depth calculated from each of these four scans is recorded and used to drive fluvial erosion and deposition.

Fluvial erosion/deposition

To represent the erosion and deposition of different grain sizes and to allow the development of an armoured surface layer, an active layer system is used similar to that of Parker (1990), Hoey and Fergusson (1994) and Toro-Escobar *et al.* (1996). CAESAR uses 12 active layers, with one for bedload, one for the surface active layer and ten further subsurface layers. The depth of the surface active layer is defined as $2D_{90}$ with the ten layers below at $4D_{90}$. Nine grain sizes are represented from 0·004 to 1·024 m in whole phi classes (-2ϕ to -10ϕ). Furthermore, the surface active layer has two additional categories representing a protective surface vegetative mat and bedrock.

When material is added to the top active layer, material is removed from this layer and added to the next layer down:

$$E_i = \left(\frac{F_i^x}{\sum F_{i-n}^x}\right)\left(\sum F_{i-n}^x - A\right) \tag{8}$$

Here E_i is the amount removed from the top layer (x) and added to the next layer down ($x+1$) of grain-size fraction i and A represents the correct thickness of the active layer ($2D_{90}$ or $4D_{90}$). For erosion or degradation, material is moved up from the lower layers according to the equation:

$$E_i = \left(\frac{F_i^{x+1}}{\sum F_{i-n}^{x+1}}\right)\left(A - \sum F_{i-n}^x\right) \tag{9}$$

Both these expressions propagate upwards and downwards respectively allowing the displacement of material through the active layers. No transfer function or filtering term is used (Hoey and Ferguson, 1994; Toro-Escobar *et al.*, 1996) as it has no temporal scaling. This representation of the river bed allows the development of an armoured surface, and the storage of deposited sediment in the stratigraphy of the other ten active layers.

The amount eroded by fluvial action from cell to cell is determined using the Einstein–Brown formulation (Einstein 1950). This was chosen as much information is available about the local hydraulic conditions

(Gomez and Church, 1989) and the total load is calculated from the sum of fractions eroded. This is well suited to the nine grain-size classes and active layer system used. The formula used here takes the form:

$$\psi = \frac{(\rho_s - \rho)^D}{\rho d S} \tag{10}$$

where ψ is the balance between the forces moving and restraining the particle, $\rho_s - \rho$ is the relative density of the submerged sediment, D is the grain size (in metres), d is the flow depth and S the energy slope. A dimensionless bedload transport rate ϕ is then calculated:

$$\phi = Q_s \sqrt{\frac{\rho}{(\rho_s - \rho) g D^3}} \tag{11}$$

ϕ is then related to ψ by the relationship plotted by Einstein (1950):

$$\phi = 40(1/\psi)^3 \tag{12}$$

A rearrangement of Equations 11 and 12 then allows q_s, the volumetric sediment load (in $m^3\ s^{-1}$), to be calculated. For each grid cell, the amount in each grain-size class that can be eroded is calculated, and removed from the active layer of the cell in question, and deposited to the active layer of the downstream cell.

Slope processes

Mass movement is represented as an instantaneous removal process. When the slope between adjacent cells exceeds a threshold (0·5 or 45 degrees), material is moved from the uphill cell to the one below until the angle is lower than the threshold. As a small slide in a cell at the base of a slope may trigger more movement uphill, the model uses an iterative procedure to check the adjacent cells until there is no more movement.

Soil creep is calculated between each cell every month of model time according to the equation:

$$Creep(a^{-1}) = \frac{S0{\cdot}01}{Dx} \tag{13}$$

For both mass movement and creep, the grain size of the moved material is accounted for by transferring material from the active layers of contributing cells to receiving. This allows fresh sediment to transfer from slopes into river channels.

Vegetation cover

Interactions between vegetation and the model are represented in two ways. Firstly, changes in land cover (e.g. deforestation) are made by altering the *m* value in the hydrological model, in turn modifying the peak and duration of a flood hydrograph for a given storm event. Secondly, a resistive turf layer can grow, protecting the surface from erosion. This is implemented by adding an extra 'turf' fraction to the surface active layer. Field shear stress measurements carried out on vegetation-covered surfaces by Prosser (1996) were used to calculate the resistivity of this layer that equates to a boulder 0·26 m in diameter. When eroded, this turf layer is removed entirely from the system and not deposited. A simple growth model is also included, so deposited alluvial surfaces (e.g. a channel bar) can become vegetated. This model will revegetate fully in ten years at a linear rate.

APPLICATION AND INITIAL CONDITIONS

For this study, CAESAR was applied to the catchment of Cam Gill Beck, North Yorkshire, UK, (Figure 2), a small, steep, upland catchment with a drainage area of 4·2 km^2. The beck descends from 700 m OD elevation to 220 m OD where it cuts through a Late Pleistocene/Early Holocene age alluvial fan on which the village of Starbotton is built, before joining the River Wharfe. The Starbotton fan is 300 m in radius and falls 10 m

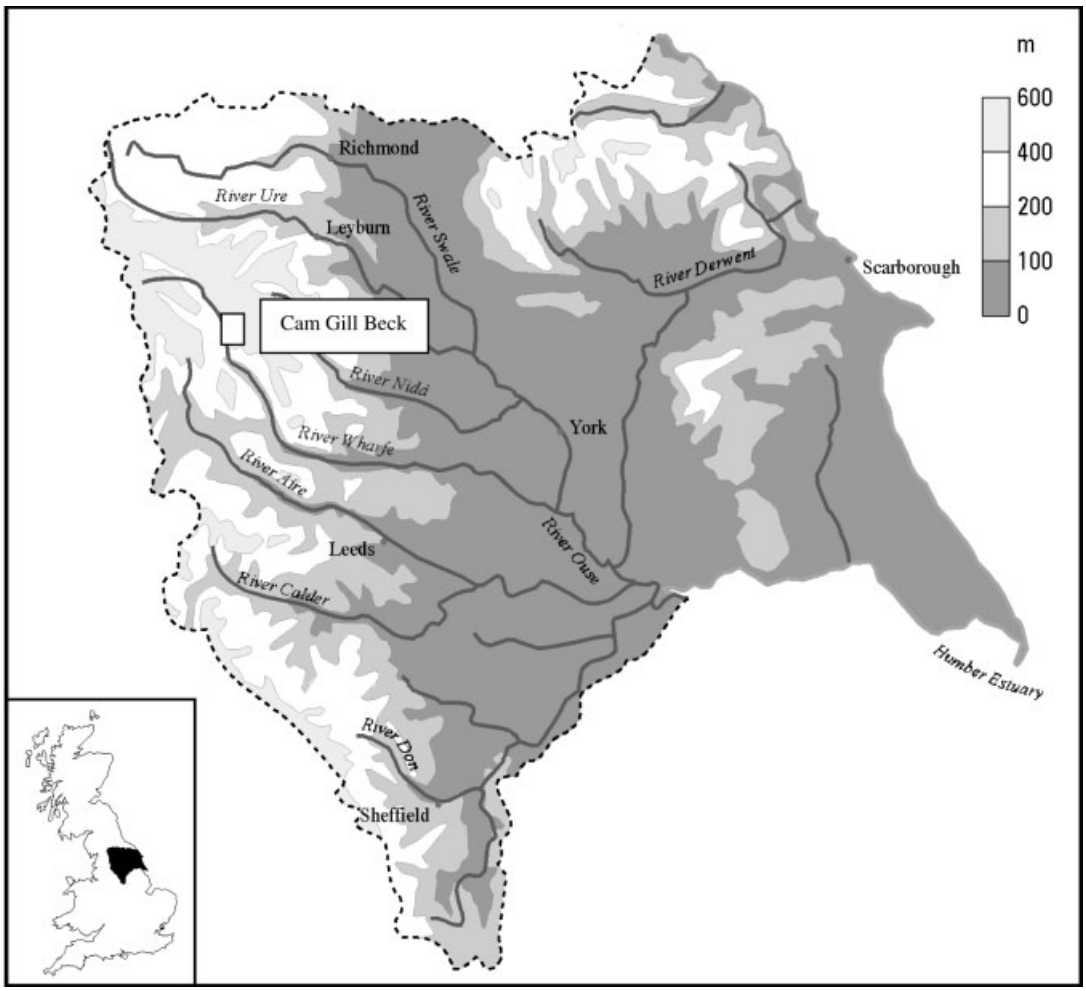

Figure 2. Relief of the Yorkshire Ouse basin, showing the location of Cam Gill Beck

from its apex to where it joins the River Wharfe. To recreate the early Holocene topography, a 3 m by 3 m resolution DEM of Cam Gill Beck was created, by digitizing 1 : 10 000 OS map contours, augmented with surveyed ground points. For the catchment upstream of the apex of the alluvial fan, this present-day topography was taken as an analogue for that 9200 cal. BP. However, as the alluvial fan was formed during this period, part of the present-day topography had to be removed. This was carried out by removing the contours that represented the fan, and extending the contours of the main valley across the fan's position, reconstructing the main valley floor some 5–10 m lower than present (Figure 3).

This surface was given a 2 m depth of regolith with the same distribution of grain-size proportions as averaged from four field measurements. This depth is considerably more than the regolith presently covering Cam Gill Beck, but is an attempt to compensate for the model not incorporating pedogenesis and weathering. The model boundary conditions were set so both water and sediment could be removed from the southern edge, but only water from the western side. This was to try to incorporate the constraining effects of the opposite valley wall, trunk stream and earlier Late Pleistocene fan deposits.

The climate input for the model is derived from a proxy wetness index from a peat bog in northern Scotland (Anderson *et al*., 1998). This sequence was resampled at 50 year intervals, and following previous applications (Coulthard *et al*., 2000, Coulthard and Macklin, 2001), normalized to values between 0·5 and 2·25 (Figure 4) to create a rainfall index. To drive the model, a ten year hourly rainfall record (1985–1995) located in Vale of

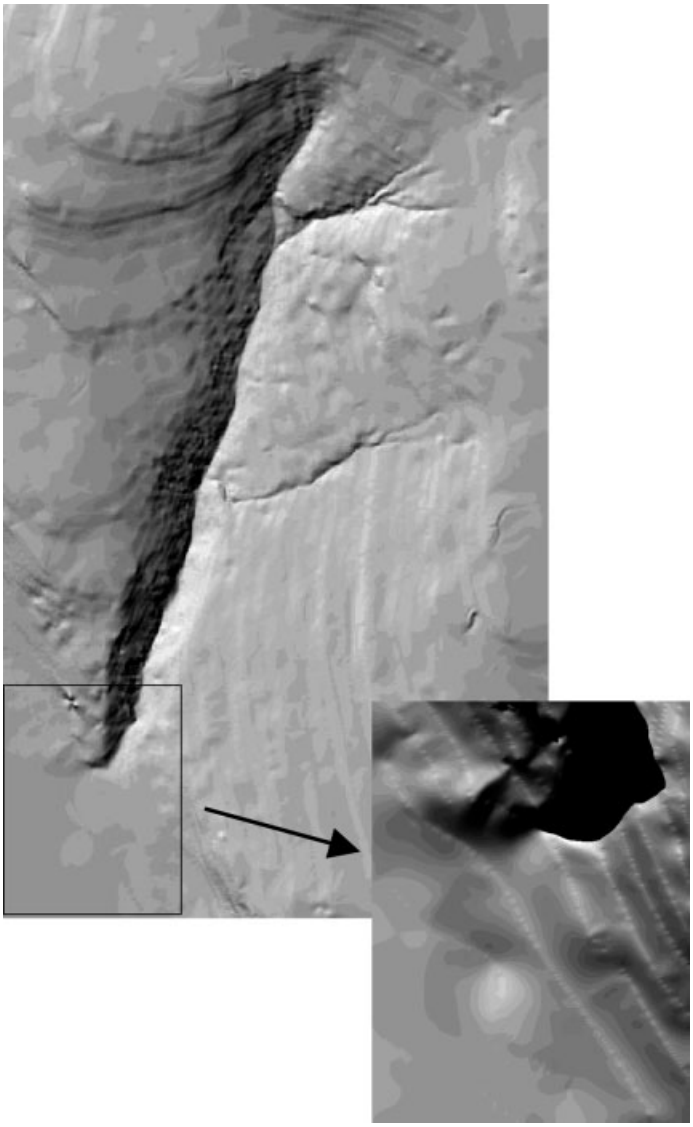

Figure 3. The DEM used for this simulation. The inset details the fan section prior to the simulation and is further detailed in Figure 9

York (SE 515370) was duplicated five times to span 50 years, and multiplied by the index, generating a proxy hourly rainfall record for the last 9200 years. This method accounts only for changes in flood magnitude; however, previous applications (Coulthard *et al*., 2000) have shown that frequency changes have a far lesser effect than magnitude. Changes in land cover are poorly documented in Wharfedale and we have used local palynological records (Tinsley, 1974; Smith, 1986) to develop a land-cover index ranging from 2 (forested) to 0·5 (grassland). This factor is divided by 100 and used as the *m* variable in the hydrological model previously described.

Defining initial conditions for grain sizes and channel dimensions throughout the catchment is a difficult task, so an initial 'spin up' time is used until the model establishes equilibrium. In this simulation, this took 200 years and can be seen by the initial sediment peak (Figures 4 and 7) as the channel established a protective armour layer. During the simulation, a grid of elevations and grain size values was saved every 50 simulated years, from which sediment discharges and topographies could be calculated.

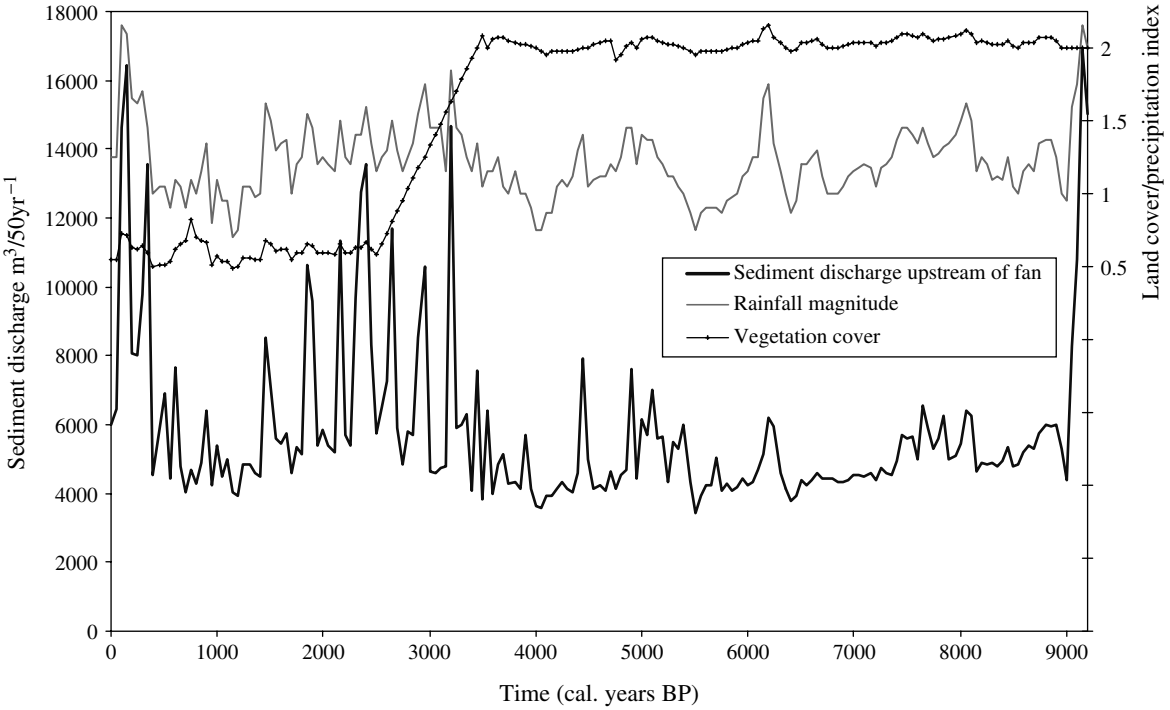

Figure 4. Sediment discharge above the alluvial fan with climate and vegetation cover

RESULTS

Figures 4–8 detail the climate and land-cover signals, the sediment discharge upstream of the alluvial fan (Figures 4 and 6), the volume of fan aggradation and the catchment sediment discharge (Figures 7 and 8). These show that changes in sediment discharge upstream of the alluvial fan are synchronous with the climate signal (Figure 4). Additionally, there is an increase in the sediment discharges during wetter periods following

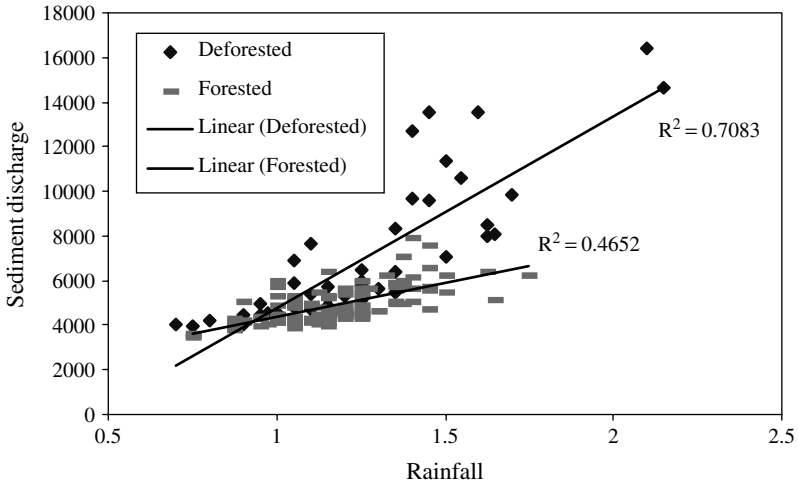

Figure 5. Scatter plot and regression lines of sediment discharge upstream of the alluvial fan and rainfall magnitude

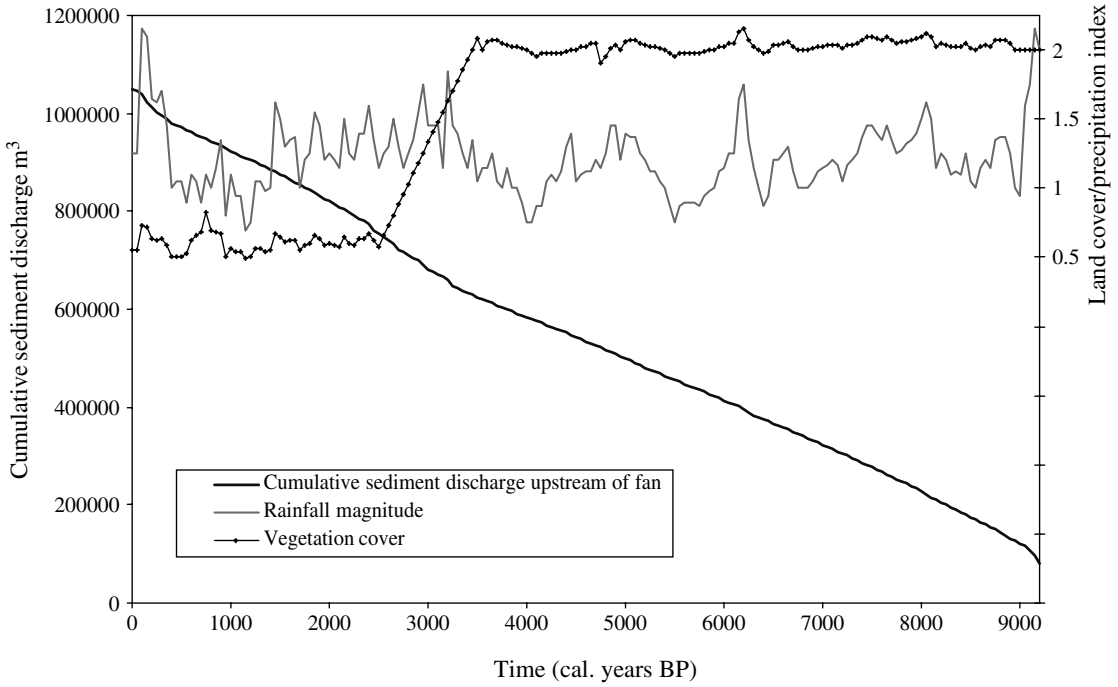

Figure 6. Cumulative total of sediment discharge above alluvial fan

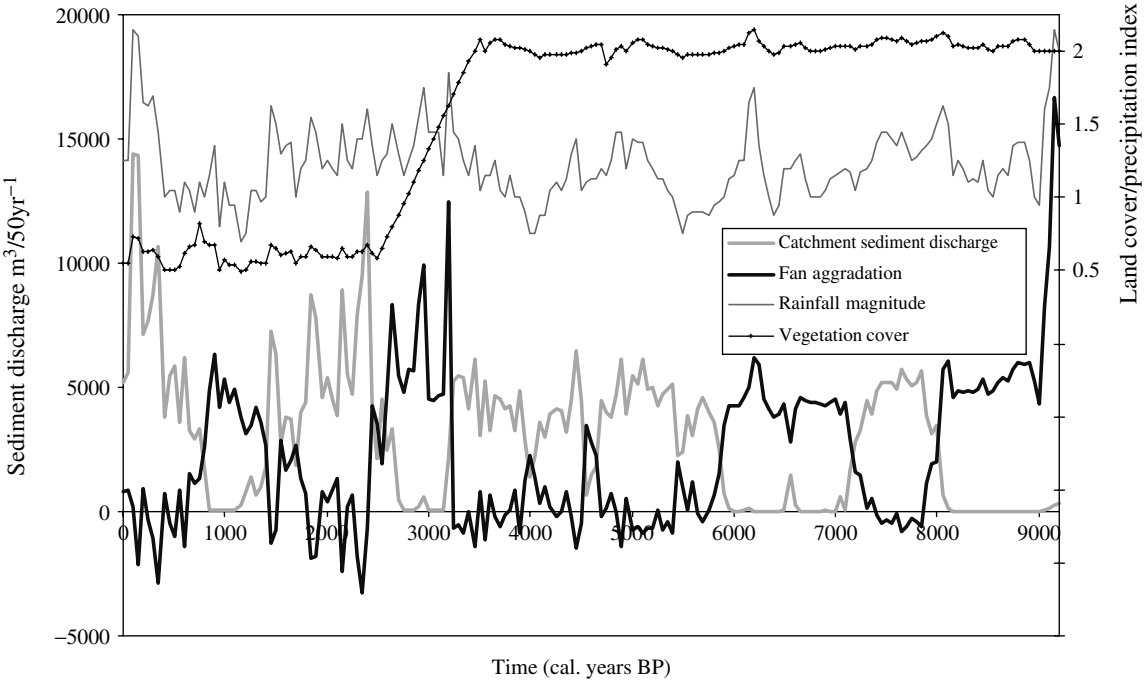

Figure 7. Fan aggradation and catchment sediment discharge

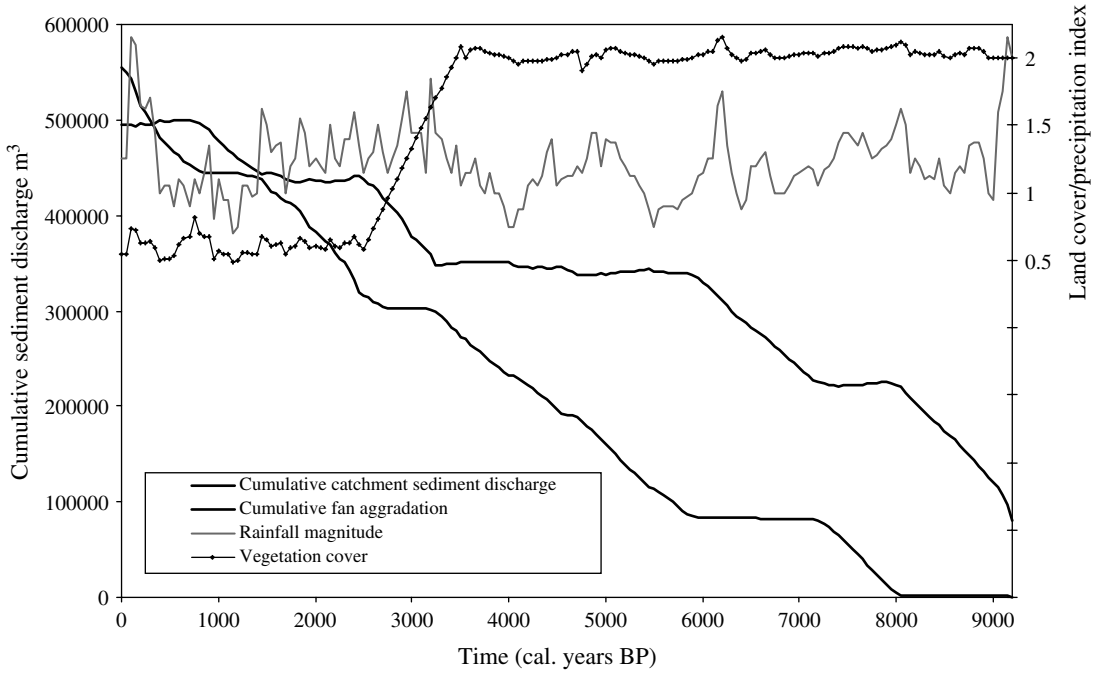

Figure 8. Cumulative chart of fan aggradation and catchment sediment discharge

deforestation (Figure 5). Furthermore, there are abrupt changes in fan sedimentation with clear switches from fan aggradation to sediment passing straight through the fan (Figures 7 and 8).

An animated view of fan evolution can be seen at http://www.interscience.wiley.com/jpages/0197-9337/sites.html showing plan views of the surface, erosion and deposition as well as cross-sections through the fan. Figure 9 shows stills from this sequence, from 9000 to 0 cal. BP at 1000 year intervals. The left-hand frame shows a shaded plan-form view of the section highlighted in Figure 3, with a 300 per cent vertical exaggeration, and the right-hand frame shows patterns of erosion and deposition in the 50 years prior to that frame.

The first four frames from 9000 to 6000 cal. BP show fan aggradation with a branching laterally mobile channel system. From 5000 to 4000 cal. BP there is incision, reduced lateral channel movement and a switch to a single channel. This is replaced at 3000 cal. BP by a major period of aggradation on the northwest section of the fan, with a switch to stability with erosion through to 2000 cal. BP, aggradation at 1000 cal. BP and incision by present day. The animated view shows these changes in far more detail. The erosion/deposition frames (Figure 9) show periods of aggradation and the multiple channels created by the sediment splaying out over the surface of the fan. Limited lateral channel movement and incision is associated with a single channel acting to transport material down across the fan and out of the catchment. The model also appears to exhibit behaviour similar to that observed in real alluvial fans. For instance, the incision and aggradation point shifts up and down the fan, creating distal and fan-head trenching and the fan also develops in a segmented fashion.

DISCUSSION

Holocene environmental change and its influence on long-term sediment discharges

This simulation shows that the sediment discharge upstream of the alluvial fan closely follows the climate signal. There is an increase in amplitude after deforestation, and the largest peaks occur when there is wet climate combined with low vegetation cover (e.g. 100–500 cal. BP). An increase in catchment sensitivity

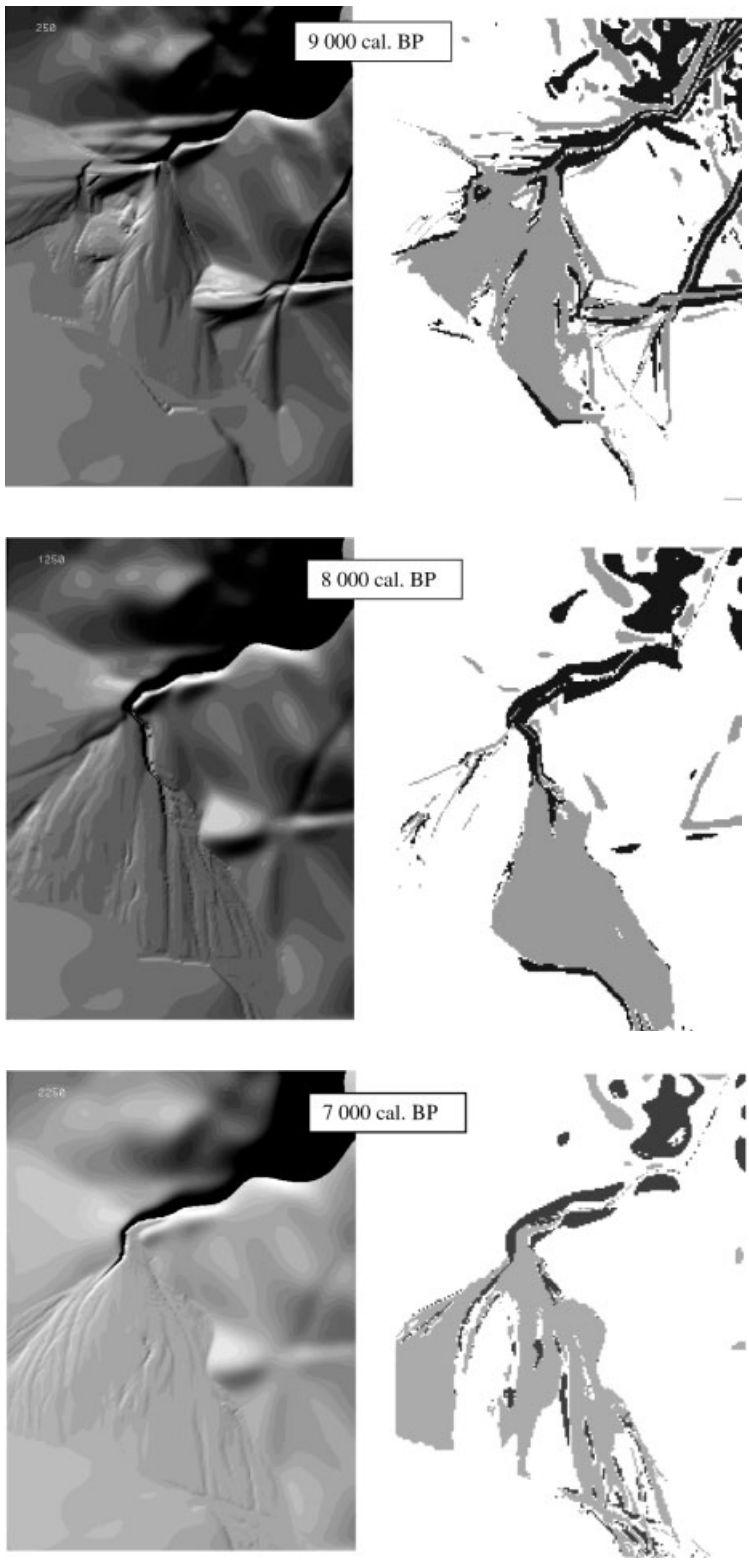

Figure 9. Topography and erosion/deposition for Cam Gill Beck alluvial fan. Dark grey areas indicate erosion, and light grey deposition

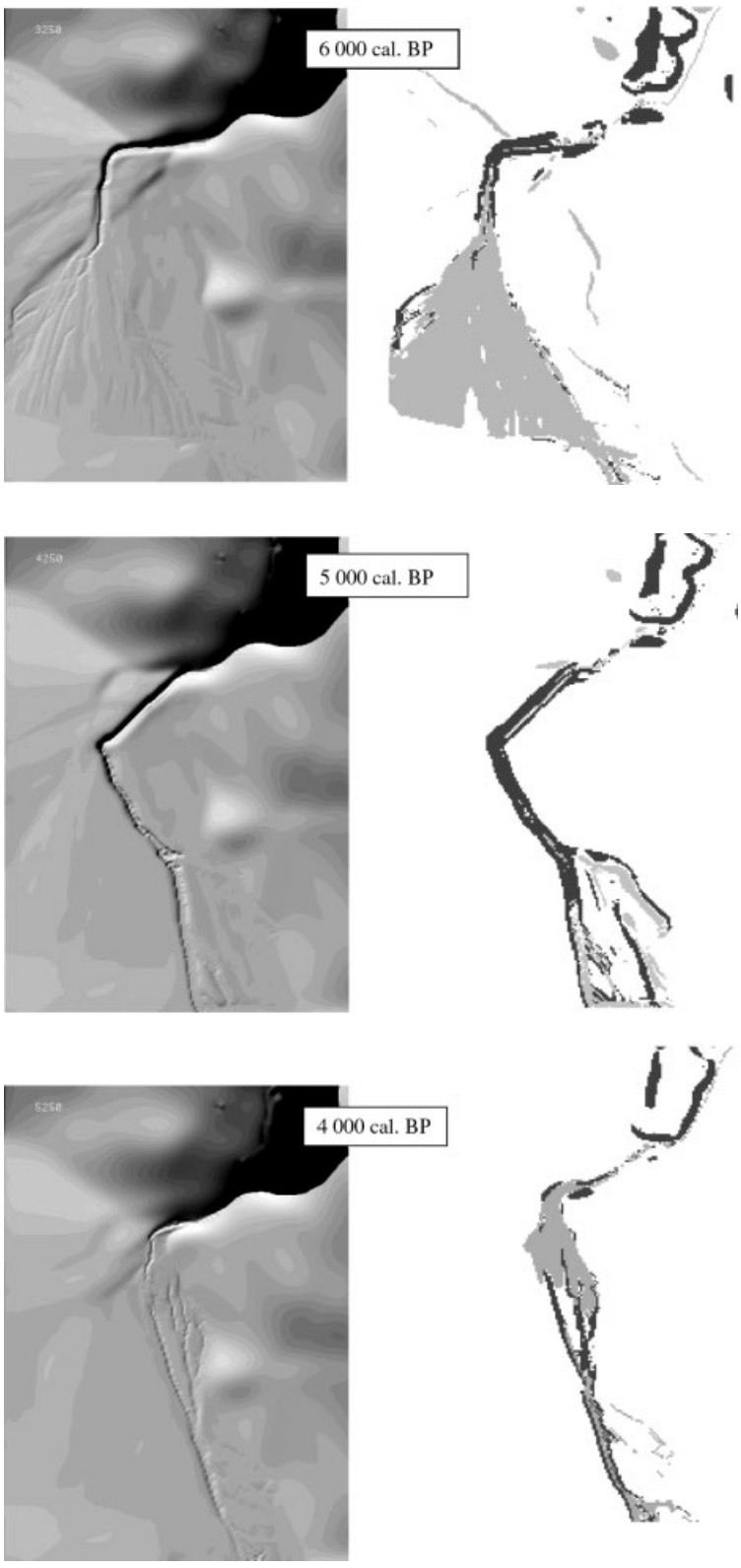

Figure 9. (*Continued*)

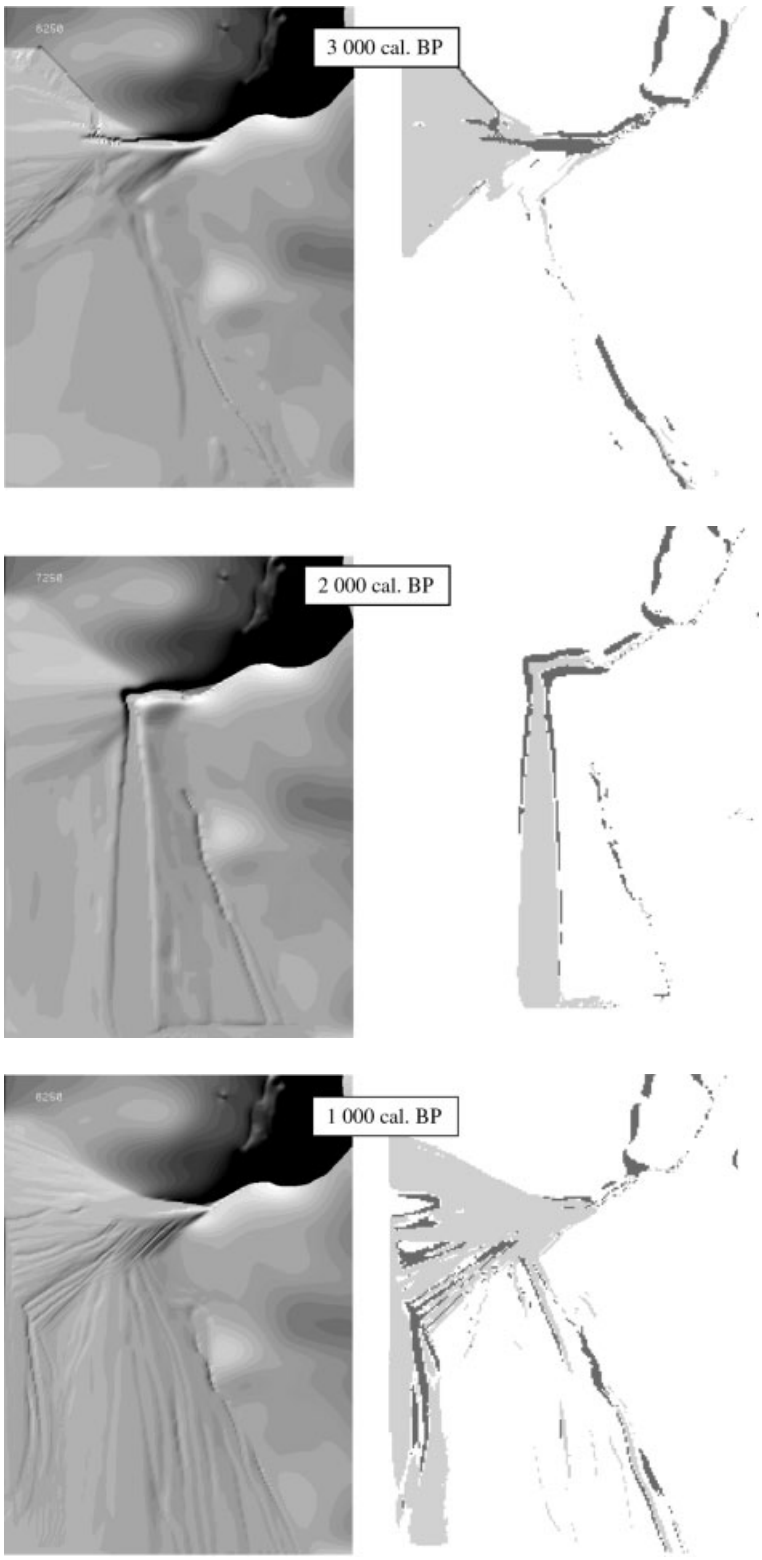

Figure 9. (*Continued*)

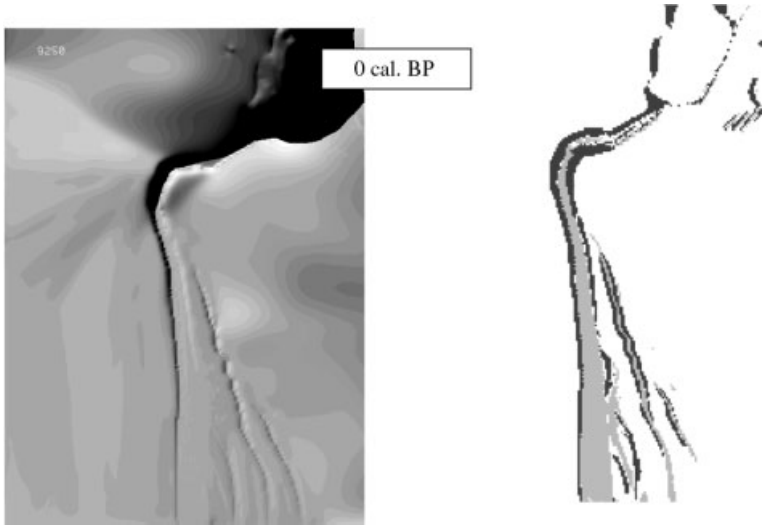

Figure 9. (*Continued*)

following land-cover change can also be shown by plotting and regressing the sediment discharge against rainfall magnitude (Figure 5). This shows that lower rainfall magnitudes (1) have a similar effect in a forested and deforested river basin. But higher rainfall magnitudes (1·5–2) can produce a far higher sediment discharge in a deforested catchment. These two lines, however, are not statistically different, but the general trend is apparent: that reducing the vegetation cover increases catchment sediment discharge in response to a similar increase in rainfall, agreeing with the findings of Coulthard *et al*. (2000) and Coulthard and Macklin (2001).

The scatter in Figure 5 suggests that the catchment responds differently to similar climate signals. This may be explained by non-linear interactions within the model (Coulthard *et al*. 1998) or by sediment supply and storage factors. For example, the peak in sediment discharge upstream of the fan at 3000 cal. BP (Figure 4) is far lower than the peaks at 2500 and 2750 cal. BP despite having a wetter climate, suggesting that the larger 3200 cal. BP peak temporarily exhausted sediment supply. This is similar to the drop in sediment discharge between peaks at 200 and 300 cal. BP, which appear greater than the corresponding change in the climate sequence.

Further evidence for the importance of sediment availability and supply is shown by plotting the cumulative sediment discharge upstream of the fan (Figure 6). Whilst Figure 4 shows a strongly fluctuating sediment discharge, the cumulative total rises steadily, showing that over longer time scales a process or processes operating at a constant rate are limiting the model response. In this simulation the only process with no temporal change in rate is soil creep. There is a change in the line at *c*. 3200 cal. BP that is caused by an increase in the size of the drainage network in response to wetter climate. This in turn enlarges the area of slope–channel coupling, increasing the volume of material fed into the channel from soil creep. This implies that upland cool maritime temperate catchments like Cam Gill Beck are supply-limited, and that over the Holocene, one of the dominant controls on sediment discharge may be soil creep. Unfortunately as soil creep operates at very low rates, it is difficult to quantify accurately and assess how these may respond to environmental change. Therefore, soil creep may be both the most important factor and the weakest link in the model parameterization. For 100-year runs the effect of soil creep is negligible, but over time scales greater than 1000 years its volumetric importance increases and a more accurate model representation may be required.

In analysing the results of this simulation, it is important to be aware that because of the detail of the model and extended length of model runs it is difficult to select accurate model parameters. For example, the initial surface of the catchment is unknown, as are the soil grain-size characteristics, and so we are forced

to use the present-day conditions as an analogue. The omission of certain processes (e.g. pedogenesis) and the use of sediment transport equations derived from larger, lower gradient streams may also influence the results. Additionally, the climate and land-use sequences are not defined with great certainty. The climate record is from Scotland not the Yorkshire Dales and, though it is very similar to Barber *et al.*'s (1994) record from northern England, it cannot be treated as a precise record of the Holocene climate at Cam Gill Beck. Similarly, the land-use history is susceptible to error, being reconstructed from regional palynological and archaeological evidence. Ironically, we have a far better proxy-record of previous climates than of our ancestors' agricultural activities. Furthermore, spatial variation in changes in vegetation, and thus hydrology, are not incorporated in this model. It is assumed that the catchment changes as a whole, by altering the m value. This may have important effects on where sediment was produced. For example, if one tributary were deforested first, it would be expected to produce sediment at different times to the rest of the catchment. Unfortunately, at present we have little knowledge of how, where and when the deforestation of Cam Gill Beck took place. However, in justification, we are for the first time trying to model the evolution of a real catchment and its fan, using the best presently available process representations and records of climate and land cover.

Alluvial fan evolution

The evolution of the Starbotton alluvial fan (Figure 9) is characterized by sudden changes in behaviour, with channel avulsions, switches from aggradation to incision, and changes in channel pattern. However, closer examination shows that periods of fan aggradation generally occur when the stream flows to the west, and incision occurs when the stream flows to the south, and this may partly be a result of the model's boundary conditions. At Starbotton, the fan spills out across the valley floor until it reaches the western valley wall and the River Wharfe. When the initial boundary conditions were designed, it was necessary to prevent material eroding from this westerly edge but include the effects of the trunk stream. To achieve this, the model allows water to escape over the western edge of the fan, but not sediment. This represents the blocking effects of the valley wall but it is not an ideal solution. The scenario this best represents is where the development of an alluvial fan is restricted on one side by an earlier fan segment. However, the influence of boundary conditions raises several key questions. In real alluvial fans what effect does the underlying topography around the fan have? What are the effects of a trunk river at the base of the fan? Does it trim the toe or does the obstruction caused by the fan block the trunk river and cause aggradation upstream? This is an area for future research, which could be explored by using CAESAR.

Although the location of aggradation may have been influenced by the boundary conditions, it is unlikely that they cause the sudden switches between fan erosion and deposition. This raises the question of what controls avulsion, incision, aggradation or changes from a multiple branching to straight channel. In this simulation, there is generally no simple relationship between changes in climate and land use, sediment discharge and fan behaviour, except at 3200 cal. BP when a wet peak in climate with high sediment discharge coincides with widespread fan aggradation. Switches in fan behaviour at 5900 and 7200 cal. BP, however, occur during dry periods, and the largest peak in catchment sediment discharge and wettest time (100 to 500 cal. BP) coincides with fan incision. Differing fan response to similar conditions of climate, land cover and sediment supply may be partly caused by processes, thresholds and instabilities within the fan itself (cf. Harvey, 1997). Furthermore, the manner in which an alluvial fan responds to environmental change, or internal forcings, will be important in controlling the connectivity between the tributary and trunk river. This simulation demonstrates how sudden shifts in sediment storage, channel position and channel pattern will affect this connectivity.

A further point of interest is that direct comparisons between the present-day and simulated fan surface show large differences (up to 8 m), particularly towards the fan apex (Figure 10). This may be due to the choice of boundary conditions, or to the model undercalculating the volume of sediment eroded from Cam Gill Beck catchment and deposited on the fan. We believe the latter cause was most likely, because we underestimated the size of the Starbotton fan at the beginning of the Holocene. This would

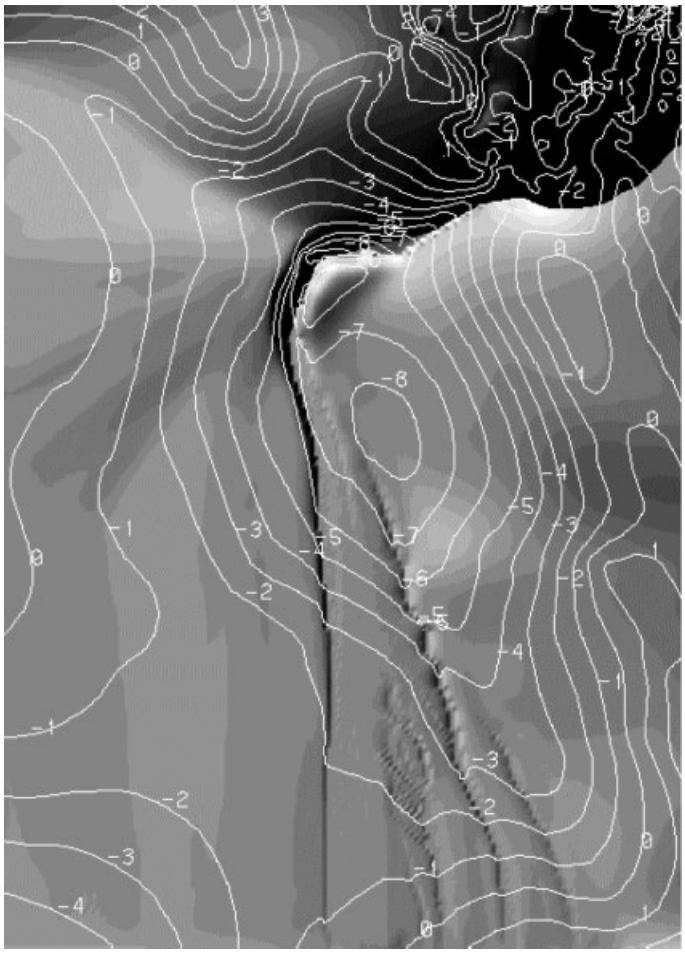

Figure 10. Contour plot of difference (in metres) between final simulation topography and present day

suggest that most of the fan was formed at the end of the late Dimlington Stadial and during the late glacial period.

CONCLUSION

The long-term simulation of the evolution of Cam Gill Beck catchment strongly suggests that both climate and land-use change influence sediment discharge, but deforestation can also dramatically increase catchment response to climate change. However, when averaged over longer periods (*c*. 1000 years), dramatic increases in sediment discharge associated with climate change are moderated by the sediment supply-limited nature of these catchments. Therefore, when examining periods longer than 1000 years, changes in the rates of diffusive slope processes such as creep may be very significant. The episodic and complex nature of the simulated development of the Starbotton alluvial fan suggests that fan evolution is not related solely to climate or land-use changes, but is also governed by sediment storage and thresholds within the system. Finally, by successfully simulating the long-term evolution of small river catchments and alluvial fans, CAESAR can help us understand fan dynamics by pinpointing critical time periods and morphological features, and can be used to predict future behaviour.

ACKNOWLEDGEMENTS

We would like to thank John Lewin for his comments on an earlier version of this paper, Adrian Harvey for notes on fan development, the two anonymous referees for very helpful comments, Joanna Schmidt of the Leeds University computing services for help with HPC facilities, and the Natural Environment Research Council for the provision of research studentship no. GT4/95/147/F to T.J.C.

REFERENCES

Anderson DE, Binney HA, Smith MA. 1998. Evidence for abrupt climatic change in northern Scotland between 3900 and 3500 calendar years BP. *The Holocene* **8**: 97–103.

Ballantyne CK. 1991. Late Holocene erosion in upland Britain: climatic deterioration or human influence? *The Holocene* **1**: 81–85.

Ballantyne CK, Whittington G. 1999. Late Holocene floodplain incision and alluvial fan formation in the central Grampian Highlands, Scotland: chronology, environment and implications. *Journal of Quaternary Science* **14**(7): 651–671.

Barber KE, Chambers FM, Maddy D, Stoneman R, Brew JS. 1994. A sensitive high resolution record of late Holocene climatic change from a raised bog in northern England. *The Holocene* **4**(2): 198–205.

Beven KJ. 1997. Topmodel: a critique. *Hydrological Processes* **11**: 1069–1085.

Beven KJ, Kirkby MJ. 1979. A physically based variable contributing-area model of catchment hydrology. *Hydrological Science Bulletin* **24**(1): 43–69.

Braun J, Sambridge M. 1997. Modelling landscape evolution on geological time scales: a new method based on irregular spatial discretization. *Basin Research* **9**: 27–52.

Coulthard TJ, Macklin MG. 2001. How sensitive are river systems to climate and land-use changes? A model based evaluation. *Journal of Quaternary Science* **16**: 346–351.

Coulthard TJ, Kirkby MJ, Macklin MG. 1998. Non-linearity and spatial resolution in a cellular automaton model of a small upland basin. *Hydrology and Earth System Sciences* **2**: 257–264.

Coulthard TJ, Kirkby MJ, Macklin MG. 1999. Modelling the impacts of Holocene environmental change on the fluvial and hillslope morphology of an upland landscape, using a cellular automaton approach. In *Fluvial Processes and Environmental Change*. Brown AG, Quine TM (eds). J. Wiley and Sons: Chichester; 31–47.

Coulthard TJ, Kirkby MJ, Macklin MG. 2000. Modelling geomorphic response to environmental change in an upland catchment. *Hydrological Processes* **14**: 2031–2045.

Einstein HA. 1950. *The bed-load function for sediment transport on open channel flows*. USDA, Soil Conservation Service, Technical Bulletin 1026.

Gomez B, Church M. 1989. An assessment of bed load sediment transport formulae for gravel bed rivers. *Water Resources Research* **25**(6): 1161–1186.

Goodchild MF, Mark DM. 1987. The fractal nature of geographic phenomena. *Annals of Association of American Geographers* **77**(2): 265–278.

Harvey AM. 1996. Holocene hillslope gully systems in the Howgill Fells, Cumbria. In *Advances in Hillslope Processes*, Volume 2. Anderson MG, Brooks SM (eds). John Wiley and Sons: Chichester; 731–752.

Harvey AM. 1997. The role of alluvial fans in arid zone fluvial systems. In *Arid Zone Geomorphology*, Thomas DSG (ed.). John Wiley and Sons: Chichester; 231–260.

Harvey AM, Renwick WH. 1987. Holocene alluvial fan and terrace formation in the Bowland fells, northwest England. *Earth Surface Processes and Landforms* **12**: 249–57.

Hoey T, Ferguson R. 1994. Numerical simulation of downstream fining by selective transport in gravel bed rivers: Model development and illustration. *Water Resources Research* **30**(7): 2251–2260.

Howard AD. 1994. A detachment limited model of drainage basin evolution. *Water resources research* **30**(7): 2261–2285.

Hutchinson MF. 1989. A new procedure for gridding elevation and stream line data with automatic removal of spurious pits. *Journal of Hydrology* **106**: 211–232.

Kirkby MJ. 1987. Modelling some influences of soil erosion, landslides and valley gradient on drainage density and hollow development. *Catena supplement* **10**: 1–11.

Macklin MG. 1999. Holocene river environments in prehistoric Britain: human interaction and impact. *Journal of Quaternary Science, Quaternary Proceedings* **7**: 521–530.

Macklin MG, Lewin J. 1993. Holocene river alluviation in Britain. *Zeitschrift fur Geomorphologie Supplement-Band* **88**: 109–122.

Macklin MG, Rumsby BT, Heap T. 1992. Flood alluviation and entrenchment: Holocene valley floor development and transformation in the British uplands. *Geological Society of America, Bulletin* **104**: 631–643.

Merrett SP, Macklin MG. 1999. Historic river response to extreme flooding in the Yorkshire Dales, Northern England. In *Fluvial Processes and Environmental Change*. Brown AG, Quine TM (eds). J. Wiley and Sons: Chichester; 345–361.

Moglen GE, Bras RL. 1995. The effect of spatial heterogeneities on geomorphic expression in a model of basin evolution. *Water Resources Research* **31**(10): 2613–2623.

Murray AB, Paola C. 1994. A cellular model of braided rivers. *Nature* **371**: 54–57.

Murray AB, Paola C. 1997. Properties of a cellular braided-stream model. *Earth Surface Processes and Landforms* **22**: 1001–1025.

Parker G. 1990. Surface based bedload transport relation for gravel rivers. *Journal of Hydraulic Research* **4**: 417–436.

Prosser IP. 1996. Thresholds of channel initiation in historical and Holocene times, south-eastern Australia. In *Advances in Hillslope Processes*, Volume 2. Anderson MG, Brooks SM (eds). John Wiley and Sons: Chichester; 687–708.

Rumsby BT, Macklin MG. 1996. River resonse to the last neoglacial (the 'Little Ice Age') in northern, western and central Europe. In *Global Continental Changes: the Context of Paleohydrology*, Branson J, Brown AG, Gregory KJ (eds). Geological Society, London, Special Publication **115**: 217–233.

Smith RT. 1986. Aspects of the soil and vegetation history of the Craven District of Yorkshire. In *Archaeology in the Pennines*, Manby TG, Turnbull P (eds). BAR British Series 158, Oxford: 3–28.

Tinsley HM. 1974. The former woodland of the Nidderdale Moors (Yorkshire) and the role of early man in its decline. *Journal of Ecology* **6**: 1–26.

Toro-Escobar CM, Parker G, Paola C. 1996. Transfer function for the deposition of poorly sorted gravel in response to streambed aggradation. *Journal of Hydraulic Research* **34**: 35–51.

Tucker GE, Slingerland RL. 1994. Erosional dynamics, flexural isostasy, and long-lived escarpments: A numerical modelling study. *Journal of Geophysical Research* **99**: 12 229–12 243.

Tucker GE, Lancaster ST, Gasparini NM, Bras RL, Rybarczyk SM. 2001. An object-oriented framework for hydrologic and geomorphic modeling using triangulated irregular networks. *Computers and Geosciences* **27**(8): 959–973.

Willgoose G, Bras I, Rodriquez-Iturbe I. 1994. Hydrogeomorphology modelling with a physically based river basin evolution model. In *Process Model and Theoretical Geomorphology*, Kirkby MJ (ed.). Wiley: Chichester; 3–22.

